

Universal Rashba Spin Precession of Two-Dimensional Electrons and Holes

Marco G. Pala,¹ Michele Governale,² Jürgen König,² and Ulrich Zülicke²

¹*Dipartimento di Ingegneria dell'Informazione, via Diotisalvi 2, I-56126 Pisa, Italy*

²*Institut für Theoretische Festkörperphysik, Universität Karlsruhe, D-76128 Karlsruhe, Germany*

(Dated: February 7, 2020)

We study spin precession due to Rashba spin splitting of electrons and holes in semiconductor quantum wells. Based on a simple analytical expression that we derive for the current modulation in a broad class of experimental situations of ferromagnet–paramagnet–ferromagnet hybrid structures, we conclude that the Datta-Das spin transistor (i) is feasible with holes and (ii) its functionality is not affected by integration over injection angles. The current modulation shows a universal oscillation period, irrespective of the different forms of the Rashba Hamiltonian for electrons and holes. The analytic formulas approximate extremely well exact numerical calculations of a more elaborate Kohn–Luttinger model.

PACS numbers: 85.75.Hh, 72.25.-b, 73.23.Ad

Transport effects based on coherent manipulation of the spin degree of freedom in low-dimensional semiconductors are currently attracting a lot of attention [1]. These studies, enabled by recent progress in nanofabrication technology to create high-quality samples, are motivated by both their interesting fundamental physics and their potential for future device applications [2]. A lot of progress in the field has been stimulated by the exploitation of spin precession due to Rashba spin-orbit (SO) coupling in 2D systems [3, 4, 5]. A prominent example is the spin-controlled field-effect transistor (spin FET) introduced by Datta and Das [6], followed by more recent proposals for novel devices utilizing Rashba SO coupling [7]. Both in the original [6] and most subsequent [10, 11, 12, 13, 14] works, a quasi-one-dimensional (1D) confinement was considered essential for proper spin-FET action. Spin precession in truly 2D electron systems was studied numerically in a number of works [8, 9].

The aim of this Letter is twofold. First, we provide a unified analytical description of spin precession for both electrons *and* holes, discussing common universal features and retaining the 2D nature of the problem. This is the most realistic case for anticipated device applications. One of our main results is illustrated in Fig. 1 where our approximate analytical expression for the current modulation in a 2D hole spin FET is compared with the full numerical result of a more elaborate Kohn–Luttinger model. Except for very small values of the distance L between the ferromagnetic contacts, the agreement is excellent. We prove analytically that the oscillation period in the 2D setup is the same as in the quasi-1D structures considered before [6, 10]. Second, we want to emphasize the utility of holes as carriers in a spin FET. The apparent disadvantage of a shorter spin life time as compared to electrons is off-set by shorter spin-precession lengths and, above all, by the possibility to use recently created [15] p-type ferromagnetic semiconductors as current injectors. Besides obvious advantages concerning

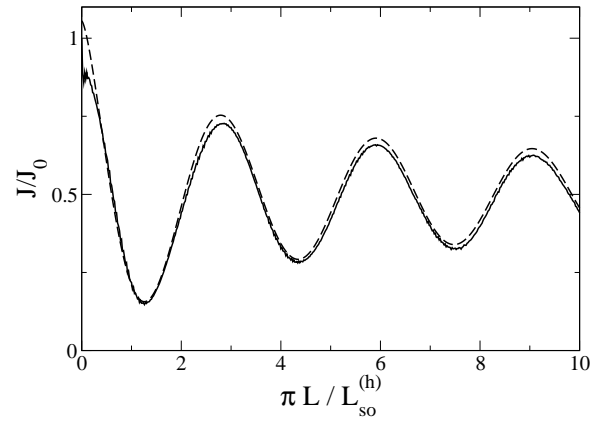


FIG. 1: Current modulation in a p-type 2D ferromagnet–paramagnet–ferromagnet hybrid system computed numerically (solid line) for a realistic system and compared with our analytic expression (dashed line). Here L is the width of the paramagnetic region, and $L_{so}^{(h)}$ the spin-precession length for holes due to the Rashba effect. The magnetizations of the two ferromagnetic regions are parallel and point in a direction perpendicular to the 2D plane of the hybrid system. For the numerical simulation we have used parameter values for a realistic GaMnAs/GaAs/GaMnAs 2D heterostructure. The hole densities are of order 10^{16} m^{-2} , $L_{so}^{(h)} \approx 300 \text{ nm}$, and the exchange field is 150 meV. There is a Fermi wave vector mismatch $k_F^{(f)}/k_{F,0} = 1.33$; and the Fermi wave vector splitting due to SO coupling is $\Delta k/k_{F,0} = 7.66 \cdot 10^{-3}$.

integrability in current semiconductor technology, such an *all-semiconductor spin FET* would circumvent the problems [16] that prevent spin injection from metallic magnets into semiconductors in the absence of a large interface barrier.

We now turn to explaining details of our calculations. A 2D hybrid system with two semi-infinite ferromagnetic contacts separated by a paramagnetic 2D stripe of width L is considered. To be specific, the extension of both ferromagnetic and nonmagnetic parts is infinite in y direction, and the nonmagnetic stripe is bounded by inter-

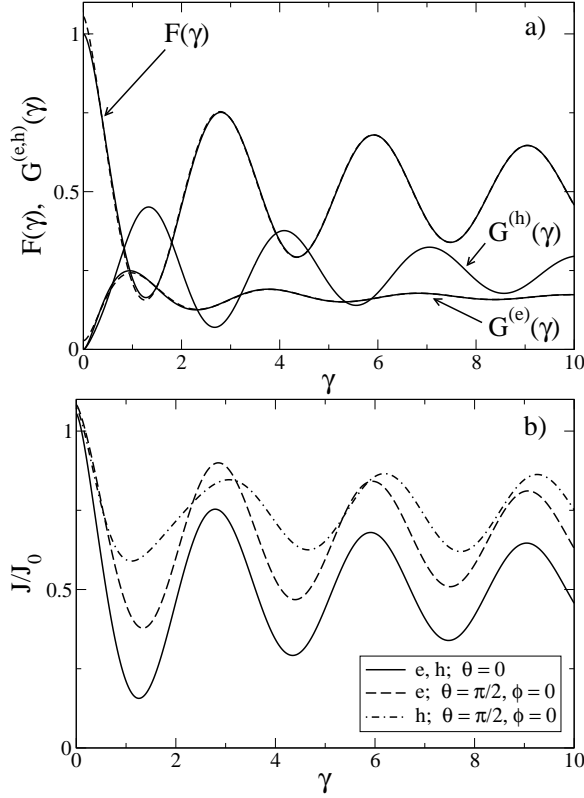


FIG. 2: a) Plot of the functions $F(\gamma)$ and $G^{(e,h)}(\gamma)$ computed numerically (solid lines) and by means of the approximated formulae given in the text (dashed line). The difference between analytical and numerical results is only barely visible for $\gamma \rightarrow 0$. b) Current density as a function of $\gamma = \pi L/L_{so}^{(e,h)}$ for different magnetization directions for both the electron and hole cases. The current is computed using the approximated expressions for $F(\gamma)$ and $G^{(e,h)}(\gamma)$.

faces to the ferromagnetic contacts at $x = 0$ and $x = L$. Due to structural inversion asymmetry in the growth (z) direction, charge carriers are subject to a spin-orbit coupling of the Rashba type [3, 5]. For electrons in the s-like conduction band, it reads $\beta_s \langle E_z \rangle (\vec{p} \times \vec{\sigma}) \cdot \hat{z}$, while for the p-like valence bands we have $\beta_p \langle E_z \rangle (\vec{p} \times \vec{J}) \cdot \hat{z}$ [17, 18]. Here, $\langle E_z \rangle$ is related to the average of the electric field in growth direction. In 2D hole quantum wells, the degeneracy of heavy-hole (HH) and light-hole (LH) valence bands at the zone center is lifted by the vertical confinement [19], and only the first HH subband (HH₁) is populated for typical 2D sheet densities. In the following, we consider only the HH₁ subband unless specified otherwise. The effective Hamiltonians for Rashba SO coupling experienced by electrons and holes are [17, 18]

$$H_{so}^{(e)} = \beta_s \langle E_z \rangle i [p_- \sigma_+ - p_+ \sigma_-] \quad (1a)$$

$$H_{so}^{(h)} = \beta_h \langle E_z \rangle i [p_-^3 \sigma_+ - p_+^3 \sigma_-], \quad (1b)$$

where $p_{\pm} = p_x \pm ip_y$ are linear combinations of momentum components, $\sigma_{\pm} = (\sigma_x \pm i\sigma_y)/2$ denote Pauli matrices, and $\beta_{s,h}$ are material parameters.

We assume identical ferromagnetic contacts having parallel magnetization M whose direction (in 3D) is described by two polar angles (θ, ϕ) . As quasi-2D ferromagnets have either easy-axis or easy-plane anisotropy, the two relevant cases are that with magnetization perpendicular to the 2D plane ($\theta = 0$) or in the plane ($\theta = \pi/2$). Assuming that there is no reflection at the interfaces between the paramagnet and the ferromagnetic contacts, we can calculate the transmission probability $T_{\theta,\phi}(\alpha)$ for an electron impinging on the first interface at an angle α . (Details are given further below.) The total current density is then $J \propto \int_{-\pi/2}^{\pi/2} T_{\theta,\phi}(\alpha) \cos(\alpha) d\alpha$. We find its expression for arbitrary magnetization direction (θ, ϕ) as

$$J = J_0 \left\{ \cos^2 \theta F(\gamma) + \sin^2 \theta \times \left[\sin^2 \phi + F(\gamma) \cos^2 \phi + G^{(e,h)}(\gamma) \cos(2\phi) \right] \right\}, \quad (2)$$

where the functions F and $G^{(e,h)}$ are shown in the panel a) of Fig. 2, and are defined explicitly below. Here $\gamma = \pi L/L_{so}^{(e,h)}$, where $L_{so}^{(e,h)} = 2\pi/\Delta k$ is the spin precession length for electrons or holes, with Δk being the difference of Fermi wave vectors for the spin-split 2D subbands:

$$L_{so}^{(e)} = \frac{\pi}{\beta_s \langle E_z \rangle} \left(\frac{\hbar^2}{m^{(e)}} \right), \quad (3a)$$

$$L_{so}^{(h)} = \frac{\pi}{2\beta_h \langle E_z \rangle} \left(\frac{\hbar^2}{m^{(h)}} \right)^2 \frac{1}{\epsilon_F}. \quad (3b)$$

Here $m^{(e,h)}$ is the effective mass for electrons/holes, and ϵ_F is the Fermi energy. Equation (3b) is valid when the Rashba spin splitting is small compared to the Fermi energy. Equation (2) is one of the central results of this Letter, and a few remarks on it are in order. Once we decide whether the carriers are electrons or holes and, hence, fix the symmetry of the band (s or p type), the current density has a universal behavior: it depends only on the ratio of the distance between the ferromagnetic contacts and the spin-precession length. Finite transparency of the interfaces and Fermi-velocity mismatch between the ferromagnetic and nonmagnetic materials will be shown below to lead only to small quantitative changes. The only difference in the functional form of the current for electrons and holes is in $G^{(e,h)}(\gamma)$ and thus appears only if the magnetization has an in-plane component. The current density Eq. (2) shows oscillations in γ with a period π , i.e. oscillations in L with a period $L_{so}^{e,h}$, that are a manifestation of spin precession in the nonmagnetic region. A few observations can be made regarding the behavior of the oscillatory part of the current density for different magnetization directions (see lower panel of Fig. 2): i) The largest oscillations of the current as a function of γ occur for magnetization perpendicular to the 2D system ($\theta = 0$); ii) In this case, electrons and holes behave exactly in the same way; iii) For in-plane magnetization

perpendicular to the interface ($\theta = \pi/2$, $\phi = 0$), the electron system exhibits a slightly larger modulation of the conductance as compared to the hole system; iv) For in-plane magnetization parallel to the interface ($\theta = \pi/2$, $\phi = \pi/2$) the conductance still shows oscillations as a function of γ (this is in contrast to the case of normal incidence), which are larger for holes. We can conclude that the oscillations of the conductance as a function of $L_{\text{so}}^{\text{e,h}}$ are not washed out by the 2D geometry of the system, i.e., by the necessity to integrate over the direction of the incoming electrons in the ferromagnet. This oscillatory behavior of the current is exploited by the spin FET. Hence, our results show analytically that the spin FET *does not* require a quasi-1D setup to work properly, and that the largest modulations of the conductance as a function of the spin precession length are obtained for magnetization perpendicular to the 2D system. Furthermore, Eq. (2) proves the feasibility of a p-type spin-FET, with holes performing even better than electrons for certain magnetization directions.

To illustrate the strategy employed to obtain the general formula Eq. (2) without inflicting lengthy algebraic manipulations to the reader, it is sufficient to show the calculation for the case of a hole system and magnetization perpendicular to the plane ($\theta = 0$). We start by calculating the probability for a plane wave in the left ferromagnet, impinging on the first interface at an angle α , to be transmitted in the second ferromagnet. We assume that only majority spins contribute to transport, hence the spin state of the incoming electron in the left ferromagnet is $|+\rangle$, where $|+\rangle$ is the spinor corresponding to spin in the $+z$ direction (the magnetization direction). We now need to write the wave function in the semiconductor. We notice first that the SO coupling Hamiltonian Eq. (1b) removes the degeneracy of HH_1 subbands. The eigenstates are still plane waves $\exp[ik(x \cos \alpha + y \sin \alpha)] \chi_{\pm}$, with spinors $\chi_{\pm} = (1/\sqrt{2})[|+\rangle \mp i \exp(i3\alpha)|-\rangle]$. The spin-split dispersion relations associated to these states read $\epsilon_{\pm} = \frac{\hbar^2}{2m^{(\text{h})}}k^2 \pm \beta_{\text{h}}\langle E_z \rangle \hbar^3 k^3$. As we study linear transport, we are interested in the states at the Fermi energy. In particular, the Fermi wave vectors for the ϵ_{\pm} bands are $k_{\text{F},\pm} = k_{\text{F},0} \mp \Delta k/2$ where $k_{\text{F},0}$ is the Fermi wave vector when no SO coupling is present. Due to translational invariance along the interface, the wave vector component parallel to the interface is conserved when going from the ferromagnet to the paramagnet. A plane wave in the ferromagnet with $\vec{k} = k_{\text{F}}^{(\text{f})}(\hat{x} \cos \alpha + \hat{y} \sin \alpha)$ gives rise to two transmitted waves with propagation directions defined by angles α_{\pm} . This effect is similar to birefringence [11, 20]: the bands ϵ_{\pm} have different Fermi wave vectors, resulting in two different propagating

directions for the transmitted waves. In the limit of weak SO coupling, i.e., $\Delta k/k_{\text{F},0} \ll 1$, the two angles read $\alpha_{\pm} = \alpha_0 \pm (1/2)(\Delta k/k_{\text{F},0}) \tan \alpha_0$, and α_0 is defined by $k_{\text{F}}^{(\text{f})} \sin \alpha = k_{\text{F},0} \sin \alpha_0$. We are now in the position to write the transmitted state in the paramagnetic strip: it simply reads $c_+ \exp[ik_{\text{F},+}(x \cos \alpha_+ + y \sin \alpha_+)] \chi_+ + c_- \exp[ik_{\text{F},-}(x \cos \alpha_- + y \sin \alpha_-)] \chi_-$. By assuming perfect transparency of the interface we can compute the coefficients c_{\pm} simply by matching the wave functions in the ferromagnet and paramagnet. At the other interface $x = L$, only the $|+\rangle$ component will be transmitted, hence the outgoing state in the right ferromagnet reads $\exp[ik_{\text{F}}^{(\text{f})}(x \cos \alpha + y \sin \alpha)] \cos[\Delta k L / (2 \cos \alpha_0)] |+\rangle$.

From that the transmission probability can be read off:

$$T_{0,\phi}(\alpha) = \cos^2 \left[\frac{\gamma}{\cos \alpha_0} \right], \quad (4)$$

where we have used the relation $\Delta k L / 2 = \gamma$, and the dependence on α is through α_0 via the relation $k_{\text{F}}^{(\text{f})} \sin \alpha = k_{\text{F},0} \sin \alpha_0$. In a similar way we can obtain the transmission probabilities for the electron case and for arbitrary magnetization direction. We find that Eq. (4) is valid for both electrons and holes. The transmission probability for in-plane magnetization reads

$$T_{\pi/2,\phi}(\alpha) = \cos^2 \left[\frac{\gamma}{\cos \alpha_0} \right] + \sin^2 [\nu_{\text{e,h}} \alpha_0 - \phi] \sin^2 \left[\frac{\gamma}{\cos \alpha_0} \right], \quad (5)$$

where $\nu_{\text{e}} = 1$ and $\nu_{\text{h}} = 3$. Finally, we can write the transmission for arbitrary magnetization direction as

$$T_{\theta,\phi}(\alpha) = \cos^2 \theta T_{0,\phi} + \sin^2 \theta T_{\pi/2,\phi}. \quad (6)$$

Equations (4–6) cease to be valid once one of the transmitted states in the paramagnet becomes evanescent and is totally reflected. This condition defines the critical angles $\alpha_{\text{c},\pm}$, that in the limit of weak SO coupling read $\alpha_{\text{c},\pm} = \frac{k_{\text{F},0}}{k_{\text{F}}^{(\text{f})}} \mp \frac{1}{2} \frac{\Delta k}{k_{\text{F}}^{(\text{f})}} \approx \frac{k_{\text{F},0}}{k_{\text{F}}^{(\text{f})}} = \alpha_{\text{c}}$.

The current density perpendicular to the interface is proportional to $\int_{-\alpha_{\text{c}}}^{\alpha_{\text{c}}} T_{\theta,\phi}(\alpha) \cos \alpha d\alpha \propto \int_{-\pi/2}^{\pi/2} \tilde{T}_{\theta,\phi}(\alpha_0) \cos \alpha_0 d\alpha_0$, where $\tilde{T}_{\theta,\phi}(\alpha_0) = T_{\theta,\phi}(\alpha(\alpha_0))$. Writing this integral with $T_{\theta,\phi}(\alpha)$ given in Eqs. (4–6), we obtain Eq. (2), where $F(\gamma)$ and $G^{(\text{e,h})}$ are

$$F(\gamma) = \frac{1}{2} \int_{-\frac{\pi}{2}}^{\frac{\pi}{2}} \cos \alpha \cos^2 \left(\frac{\gamma}{\cos \alpha} \right) d\alpha, \quad (7)$$

$$G^{(\text{e,h})}(\gamma) = \frac{1}{2} \int_{-\frac{\pi}{2}}^{\frac{\pi}{2}} \cos \alpha \sin^2 (\nu_{\text{e,h}} \alpha) \sin^2 \left(\frac{\gamma}{\cos \alpha} \right) d\alpha. \quad (8)$$

We have obtained an approximate analytical solution of Eqs. (7) and (8) that is valid unless γ is very small:

$$F(\gamma) = \frac{\pi\sqrt{2}}{8} \left\{ (4\gamma - 1)S\left(2\sqrt{\frac{\gamma}{\pi}}\right) + (-4\gamma + 1)C\left(2\sqrt{\frac{\gamma}{\pi}}\right) + 2\sqrt{\frac{\gamma}{\pi}}[\cos(2\gamma) + \sin(2\gamma)] + 1 + \frac{4}{\pi\sqrt{2}} \right\}, \quad (9)$$

$$G^{(e,h)}(\gamma) = \sqrt{2}\pi \left\{ P^{(e,h)}(\gamma)C\left(2\sqrt{\frac{\gamma}{\pi}}\right) + P^{(e,h)}(-\gamma)S\left(2\sqrt{\frac{\gamma}{\pi}}\right) - \sqrt{\frac{\gamma}{\pi}}[Q^{(e,h)}(\gamma)\cos(2\gamma) + Q^{(e,h)}(-\gamma)\sin(2\gamma)] + M^{(e,h)}(\gamma) \right\}, \quad (10)$$

where C and S are cosine and sine Fresnel integrals [21], respectively, and

$$P^{(e)}(\gamma) = \frac{2}{3}\gamma^3 - \frac{1}{2}\gamma^2 + \frac{1}{8}\gamma + \frac{1}{32}, \quad P^{(h)}(\gamma) = \frac{61}{315}\gamma^7 - \frac{16}{45}\gamma^6 + \frac{4}{3}\gamma^5 - \gamma^4 + \frac{11}{12}\gamma^3 - \frac{7}{16}\gamma^2 + \frac{9}{64}\gamma + \frac{13}{256} \quad (11a)$$

$$Q^{(e)} = \frac{1}{3}\gamma^2 + \frac{1}{6}\gamma + \frac{1}{16}, \quad Q^{(h)} = \frac{32}{315}\gamma^6 + \frac{16}{105}\gamma^5 + \frac{218}{315}\gamma^4 + \frac{34}{105}\gamma^3 + \frac{11}{24}\gamma^2 + \frac{7}{48}\gamma + \frac{13}{128} \quad (11b)$$

$$M^{(e)}(\gamma) = \frac{1}{2}\gamma^2 - \frac{1}{32} + \frac{1}{6\pi\sqrt{2}}, \quad M^{(h)}(\gamma) = \frac{16}{45}\gamma^6 + \gamma^4 + \frac{7}{16}\gamma^2 + \frac{17\sqrt{2}}{140\pi} - \frac{13}{256}. \quad (11c)$$

In Fig. 2 we compare the approximate results Eqs. (9) and (10) with the integrals of Eqs. (7) and (8). The approximate formulae work extremely well: the largest errors are for $\gamma = 0$, and hence not in the region of physical interest, and the errors decrease monotonically with increasing γ . The *relative* errors for $\gamma = \pi$, i.e., after a full precession, are of order 10^{-3} [22].

We have derived the above results for transmission probabilities [Eqs. (6)] and the current density [Eq. (2)] making use of several approximations, such as perfectly transparent interfaces and, in the hole case, the truncation to the lowest heavy-hole subband. We now test the accuracy of our approximate results by comparing them to a more realistic model for the hole system which is the more complicated one. Both the magnetic and nonmagnetic parts of the hybrid system are modelled by a 4×4 Kohn-Luttinger Hamiltonian with HH and LH bands. The confinement in the growth direction is treated by means of the envelope-function approximation. The ferromagnetic contacts are described within the Stoner approach by an exchange field. Calculation of the current density yields the result shown in Fig. 1 as a solid line. Excellent agreement between our approximate analytical results and the exact numerical curve is apparent (note that for the latter a Fermi wave vector mismatch across the interface is present.) The only effect of nonideal interfaces on the current modulation is a renormalization of its amplitude J_0 .

In conclusions, we have studied spin precession in electron and hole system, finding a universal expression for the current in a spin FET geometry. The full 2D nature of the problem is retained. Our results show that the current through the system is determined only by the common magnetization direction in the ferromagnets and by the ratio of the distance between the ferromagnetic contacts and the spin-precession length.

This work was supported by DFG through the Center for Functional Nanostructures. M. P. acknowledges support from the IST NanoTCAD project (EC contract IST-1999-10828). We thank P. Mastroia for suggesting a method to evaluate the integrals in Eqs. (7) and (8).

-
- [1] *Semiconductor Spintronics and Quantum Computation*, D. D. Awschalom, D. Loss, and N. Samarth (eds.), Series Nanoscience and Technology (Springer, Berlin, 2002).
 - [2] S. A. Wolf *et al*, Science **294**, 1488 (2001).
 - [3] E. I. Rashba, Fiz. Tverd. Tela (Leningrad) **2**, 1224 (1960), [Sov. Phys. Solid State **2**, 1109 (1960)].
 - [4] Y. A. Bychkov and E. I. Rashba, J. Phys. C **17**, 6039, (1984).
 - [5] G. Lommer, F. Malcher, and U. Rössler, Phys. Rev. Lett. **60**, 728 (1988).
 - [6] S. Datta and B. Das, Appl. Phys. Lett. **56**, 665, (1990).
 - [7] E. A. de Andrada e Silva and G. C. La Rocca, Phys. Rev. B **59**, R15583 (1999); J. Nitta, F. E. Meijer, and H. Takayanagi, Appl. Phys. Lett. **75**, 695 (1999); A. A. Kiselev and K. W. Kim, Appl. Phys. Lett. **78**, 775, (2001); T. Koga *et al.*, Phys. Rev. Lett. **88**, 126601 (2002); M. Governale *et al.*, Phys. Rev. B **65**, 140403(R) (2002); J. C. Egues, G. Burkard, and D. Loss, Phys. Rev. Lett. **89**, 176401 (2002).
 - [8] A. Bournel, P. Dolfus, P. Bruno, and P. Hesto, Eur. Phys. J. AP **4**, 1 (1998); T. P. Pareek and P. Bruno, Phys. Rev. B **65**, 241305 (2002).
 - [9] O. E. Raichev and P. Debray, Phys. Rev. B **65**, 085319 (2002).
 - [10] F. Mireles, and G. Kirczenow, Phys. Rev. B **64**, 024426 (2001).
 - [11] T. Matsuyama *et al.* Phys. Rev. B **65**, 155322 (2002).
 - [12] M. Governale, and U. Zülicke, Phys. Rev. B **66**, 073311 (2002).
 - [13] J. C. Egues, G. Burkard, and D. Loss, cond-mat/0209682.
 - [14] W. Häusler, Phys. Rev. B **63**, 121310(R) (2001).

- [15] H. Ohno, *Science* **281**, 951 (1998).
- [16] G. Schmidt et al., *Phys. Rev. B* **62**, R4790 (2000).
- [17] R. Winkler, *Phys. Rev. B* **62**, 4245 (2000).
- [18] R. Winkler *et al.*, *Phys. Rev. B* **65**, 155303 (2002).
- [19] W. W. Chow, S. W. Koch, and M. Sargent III, in *Semiconductor Laser Physics* (Springer-Verlag, Berlin), pp. 179-211.
- [20] V. Marigliano Ramaglia *et al.*, cond-mat/0203569.
- [21] M. Abramowitz and I. A. Stegun, *Handbook of Mathematical Functions* (Dover Publications, New York, 1974).
- [22] The absolute errors at $\gamma = 0$ for $F(\gamma)$, $G^{(e)}(\gamma)$, and $G^{(h)}(\gamma)$ are, respectively, $\pi/(4\sqrt{2}) - 1/2 \approx 5.54 \cdot 10^{-2}$, $1/6 - \pi/(16\sqrt{2}) \approx 2.78 \cdot 10^{-2}$, and $13/70 - 13\pi/(128\sqrt{2}) \approx 1.72 \cdot 10^{-2}$. For $\gamma = \pi$, the relative errors for $F(\gamma)$, $G^{(e)}(\gamma)$, and $G^{(h)}(\gamma)$ are, respectively, $1.83 \cdot 10^{-3}$, $7.49 \cdot 10^{-3}$, and $7.19 \cdot 10^{-4}$.